HHS Public Access

Author manuscript

Cancer Res. Author manuscript; available in PMC 2020 August 25.

Published in final edited form as:

Cancer Res. 2018 March 01; 78(5): 1266–1274. doi:10.1158/0008-5472.CAN-17-1718.

Deletion of the von Hippel-Lindau Gene in Hemangioblasts Causes Hemangioblastoma-like Lesions in Murine Retina

Herui Wang[1,2], **Matthew J. Shepard**[2,3], **Chao Zhang**[2,4], **Lijin Dong**[5], **Dyvon Walker**[2], **Liliana Guedez**[5], **Stanley Park**[5], **Yujuan Wang**[5,6], **Shida Chen**[5,6], **Ying Pang**[7], **Qi Zhang**[1], **Chun Gao**[5], **Wai T. Wong**[5], **Henry Wiley**[5], **Karel Pacak**[7], **Emily Y. Chew**[5], **Zhengping Zhuang**[1,2], **Chi-Chao Chan**[5]

[1]Neuro-Oncology Branch, Center for Cancer Research, National Cancer Institute, NIH, Bethesda, Maryland. [2]Surgical Neurology Branch, National Institute of Neurological Disorders and Stroke, NIH, Bethesda, Maryland. [3]Department of Neurologic Surgery, University of Virginia Health System, Charlottesville, Virginia. [4]Department of Orthopedics, Xinqiao Hospital, Third Military Medical University, Chongqing, China. [5]National Eye Institute, NIH, Bethesda, Maryland. [6]State Key Laboratory of Ophthalmology, Zhongshan Ophthalmic Center, Sun Yat-sen University, Guangzhou, China. [7]Eunice Kennedy Shriver National Institute of Child Health and Human Development, NIH, Bethesda, Maryland.

Abstract

von Hippel-Lindau (VHL) disease is an autosomal-dominant tumor predisposition syndrome characterized by the development of highly vascularized tumors and cysts. LOH of the *VHL* gene results in aberrant upregulation of hypoxia-inducible factors (HIF) and has been associated with tumor formation. Hemangioblastomas of the central nervous system and retina represent the most prevalent VHL-associated tumors, but no VHL animal model has reproduced retinal capillary hemangioblastomas (RCH), the hallmark lesion of ocular VHL. Here we report our work in developing a murine model of VHL-associated RCH by conditionally inactivating *Vhl* in a

Corresponding Authors: Chi-Chao Chan, NIH/National Eye Institute, 10 Center Drive, 10/10S247, Bethesda, MD 20892-1857. Phone: 301-905-6460; Fax: 301-480-1122; chanc@nei.nih.gov.

Authors' Contributions

Conception and design: H. Wang, L. Dong, S. Park, K. Pacak, E.Y. Chew, Z. Zhuang, C.-C. Chan

Development of methodology: H. Wang, L. Dong, L. Guedez, S. Park, Y. Wang, C. Gao, W.T. Wong, E.Y. Chew, Z. Zhuang, C.-C. Chan

Acquisition of data (provided animals, acquired and managed patients, provided facilities, etc.): H. Wang, M.J. Shepard, C. Zhang, L. Guedez, S. Park, S. Chen, Y. Pang, K. Pacak, E.Y. Chew, C.-C. Chan

Analysis and interpretation of data (e.g., statistical analysis, biostatistics, computational analysis): H. Wang, M.J. Shepard, L. Dong, Y. Wang, Q. Zhang, W.T. Wong, H. Wiley, E.Y. Chew, Z. Zhuang, C.-C. Chan

Writing, review, and/or revision of the manuscript: H. Wang, M.J. Shepard, L. Dong, D. Walker, L. Guedez, S. Chen, Y. Pang, Q. Zhang, W.T. Wong, H. Wiley, K. Pacak, E.Y. Chew, Z. Zhuang, C.-C. Chan

Administrative, technical, or material support (i.e., reporting or organizing data, constructing databases): H. Wang, C. Zhang, L. Guedez, Y. Wang, Y. Pang, Q. Zhang, C.-C. Chan

Study supervision: Z. Zhuang, C.-C. Chan

Disclosure of Potential Conflicts of Interest

No potential conflicts of interest were disclosed.

The costs of publication of this article were defrayed in part by the payment of page charges. This article must therefore be hereby marked *advertisement* in accordance with 18 U.S.C. Section 1734 solely to indicate this fact.

hemangioblast population using a *Scl*-Cre-ERT2 transgenic mouse line. In transgenic mice carrying the conditional allele and the *Scl*-Cre-ERT2 allele, 64% exhibited various retinal vascular anomalies following tamoxifen induction. Affected *Vhl*-mutant mice demonstrated retinal vascular lesions associated with prominent vasculature, anomalous capillary networks, hemorrhage, exudates, and localized fibrosis. Histologic analyses showed RCH-like lesions characterized by tortuous, dilated vasculature surrounded by "tumorlet" cell cluster and isolated foamy stromal cells, which are typically associated with RCH. Fluorescein angiography suggested increased vascular permeability of the irregular retinal vasculature and hemangioblastoma-like lesions. *Vhl* deletion was detected in "tumorlet" cells via microdissection. Our findings provide a phenotypic recapitulation of VHL-associated RCH in a murine model that may be useful to study RCH pathogenesis and therapeutics aimed at treating ocular VHL.

Introduction

von Hippel-Lindau (VHL) disease is a highly penetrant, autosomal-dominant tumor predisposition syndrome characterized by the formation of retinal and central nervous system (CNS) hemangioblastomas, clear cell renal carcinomas, endolymphatic sac tumors of the middle ear, pheochromocytomas, as well as pancreatic and hepatic cysts (1–4). Retinal capillary hemangioblastomas (RCH) is a benign tumor of the retina that represents the first manifestation of the disease in upwards of 50% of VHL patients (1). RCH account for significant visual loss in affected individuals with 25% of affected globes harboring visual acuity less than 20/160 (5). The pathogenesis of VHL-related RCH is believed to be secondary to abberant upregulation of hypoxia-inducible factors (HIF), whose degradation is mediated by the VHL protein (pVHL; refs. 2, 6, 7).

Biallelic mutations in the von Hippel-Lindau tumor suppressor gene (*VHL*) located on chromosome 3p25 are responsible for the pathogenesis of VHL disease, consistent with the Knudson "two-hit" hypothesis (1, 2). Approximately 60%–70% of *VHL* mutations cause truncation of pVHL by nonsense, insertion and/or deletion, or splice site mutations (8). VHL protein binds with elongin B, elongin C, and cullin 2 thereby forming the VCB-Cul2 complex that under normoxia condition ubiquitinates the α subunit of HIF1 and HIF2, which leads to their degradation in the proteasome (2, 7). However, in the case of decreased pVHL, HIFα subunits are not degraded, leading to the inappropriate upregulation of VEGF, carbonic anhydrase 9 (CA9), and other HIF target genes that are believed to be important for tumor formation (1–3, 7).

To date, no murine model has been developed to comprehensively study VHL disease. Conventional biallelic *Vhl* knockout mice are embryonically lethal (9). Conditional knockout strains have been established via tissue-specific inactivation of *Vhl* in the kidney, liver, genitourinary tract, or pancreas (9–14). Although these murine models have aided in the study of VHL disease, they have not allowed for the study of CNS or retinal hemangioblastomas (5). Because of the high rates of significant ocular morbidity in VHL disease, further investigation into RCH pathophysiology and the development of novel treatment strategies are needed. As such, the development of an RCH animal model would be transformative (5, 9).

pVHL and HIF1α have been previously shown to be critical in regulating the transition from fetal to adult circulatory system in retina (15). Conditional knockout of *Vhl* in murine retinal progenitor under control of the *Pax6* retina-specific regulatory element, α-promoter (*α-Cre*) led to the persistence of retinal hyaloid vasculature, but not the formation of RCH-like lesions, suggesting that neural retinal progenitor cells are not the primordial cell of origin for RCH (9, 15). Our group previously reported that VHL-related hemangioblastomas in the CNS express brachyury, stem cell leukemia (SCL), and fetal liver kinase 1 (FLK1) and can be differentiated into multiple hematopoietic cell lineages, suggesting that VHL-related hemangioblastomas are derived from mesoderm-derived, embryonically arrested hemangioblasts (5, 9, 16).

In this study, we used *Scl*-Cre-ERT2 transgenic mice to conditionally knockout *Vhl* in hemangioblast-derived cells after birth. Following induction, 64% (18/28) of the transgenic mice carrying the conditional allele and the *Scl*-Cre-ERT2 allele exhibited manifestations of ocular VHL. This included the development of RCH-like lesions characterized by tortuous, dilated vasculature sur- rounded by “tumorlet” cells. Laser capture microdissection showed that RCH-like lesions carry *Vhl* deletion. Our results support the hypothesis that retinal hemangioblastomas are derived from hemangioblast cell lineage. Furthermore, we believe that this *Vhl* conditional knockout mouse model will be of critical importance for the future study of RCHs.

Materials and Methods

Mouse strains

$Vhl^{F/F}$ mice were purchased from the Jackson Laboratory (stock no. 012933; ref. 11). *Scl*-Cre-ERT2 transgenic mice were kindly provided by Telethon Institute for Child Health Research in Australia under a NIH material transfer agreement (MTA). *Rosa26*-AP reporter mice were kindly provided by Dr. Tudor Badea at National Eye Institute (NEI; Bethesda, MD). All mouse experiments were performed in accordance with protocols approved by the Animal Care and Use Committee of NIH (Bethesda, MD).

Tamoxifen administration

Two-week-old mice of indicated genotype were injected intraperitoneally with 50 μL of tamoxifen solution (Sigma, 10 mg/mL in corn oil) for 5 consecutive days. Phenotypic and molecular analysis of the mutant and littermate control mice start at least 2 months after tamoxifen treatment.

Alkaline phosphatase staining

Alkaline phosphatase (AP) staining of the mouse retina and brain was performed as reported previously (17). Briefly, the eye and brain were collected after transcardiac perfusion with 4% paraformaldehyde in PBS. The brains were set in 3% low-melting point agarose in PBS and a series of 300-μm sections were cut with a vibratome. Retinas were carefully dissected from eyes and gently flattened with a plastic mesh under Leica dissecting microscope. Heat-inactivated tissues (69°C for 90 minutes) were reacted in NBT/BCIP for several hours to overnight at room temperature with gentle agitation. After washing and postfixation, tissues

were dehydrated with a graded ethanol series, and clarified in 2:1 benzylbenzoate:benzyl alcohol (BBBA). Tissues were returned to ethanol for long-term storage.

Western blot analysis

Retinas were dissected from 2.5-month-old tamoxifen-treated conditional knockout (*Scl*-Cre-ERT2; $Vhl^{F/F}$) and littermate control mice ($Vhl^{F/F}$) for protein extraction with proteinase inhibitor-containing RIPA lysis buffer. Extracted protein was subjected to NuPAGE™ 4%–12% Bis-Tris Protein Gels (Thermo Fisher Scientific), transferred to nitrocellulose membrane (iBlot2; Invitrogen), probed with anti-VHL (sc-5575, 1:1,000; Santa Cruz Biotechnology), anti-CA9 (PA1–16592, 1:1,000; Thermo Fisher Scientific), and anti-β-actin (A5441, 1:1000; Sigma). Species-specific horse-radish peroxidase-conjugated secondary antibody (1:1,000; Kindle Biosciences) was detected by enhanced chemiluminescence substrate (R1004; Kindle Biosciences) and imaged by KwikQuant Imager (D1001; Kindle Biosciences).

Funduscopy

Funduscopy examinations were performed with a custom made Xenon Nova Storz Endoscope attached with a Nikon D90 camera as described previously (18). In summary, 28 tamoxifen-treated *Scl-Cre-ERT2;* $Vhl^{F/F}$mice including 11 male and 17 female mice were examined by funduscopy for phenotypic analysis. Eight tamoxifen-treated $Vhl^{F/F}$mice including three male and five female mice were also examined as the littermate control. The funduscopy images were evaluated by C.-C. Chan (NEI, an American board-certified ophthalmologist, ophthalmic pathologist) and E.Y. Chew (NEI, an American board-certified ophthalmologist, retinal specialist).

Fluorescein angiography

Mice were injected intraperitoneally with Fluorescein AK-FLUOR (100 mg/mL; Akorn) at 100 μg/g (body weight). After 10 minutes, fluorescein angiography (FA) of the retina was performed using a Phoenix Micron III retinal imaging system (Phoenix Research Labs), according to the manufacturer's instruction. Both bright-field and fluorescence images were taken. In summary, four 4- to 6-month-old *Vhl* CKO mice with dilated tortuous vessels and three littermate controls were examined. The FA images were evaluated by E.Y. Chew.

Histology

Enucleated eyes were fixed in 10% formalin and processed for routine histology at the Histology Core of the National Eye Institute (NEI; Bethesda, MD). Hematoxylin and eosin staining was performed on paraffin- or plastic-embedded sections (5 μm). IHC staining was performed using anti-CD31 (M0823, 1:50; Agilent), anti-SCL (sc-393287, 1:100; Santa Cruz Biotechnology), and anti-VEGF (ab52917, 1:100; Abcam). Pathologic analysis was performed by C.-C. Chan.

Microdissection and PCR

Microdissection of "tumorlet" cells was performed with the Zeiss PALM laser capture microdissection system, according to the manufacturer's instruction. We performed nested

PCR (OneTaq DNA Polymerase, NEB) to detect *Vhl* deletion with the DNA extracted from the laser-captured samples. The primers for the first PCR round are mVhl-F1 and mVhl-B1. The primers for the second PCR rounds are mVhl-F1 and mVhl-B2. We also amplified Cre transgenic allele (Cre-F1 and Cre-R2) with the same amount of microdissection DNA to insure adequate DNA was isolated for both “tumorlet” and control areas.

The primers used in this manuscript are listed as follows.

Genotyping PCR:

mVhl-GT-F1: 5′-AGAGTCCAGTGAGTCGCAGGG-3′.

mVhl-GT-F2: 5′-CGATCTTTCTGCCTTCGCCACT-3′.

mVhl-GT-B1: 5′-TAGCCATCCAGTCATGACACTG-3′.

Microdissection PCR:

mVhl-F1: 5′-GAAAGTGTCCGATCCCCTGG-3′.

mVhl-B1: 5′-ACAGCCCCAATTCACTACGG-3′.

mVhl-B2: 5′-TAGCCATCCAGTCATGACACTG-3′.

Cre-F1: 5’-GGAAAATGCTTCTGTCCGTTTG-3’.

Cre-R2: 5’-TTGGTCCAGCCACCAGCTTG-3’.

Results

Inducible *Vhl* deletion in hemangioblast-derived tissues

The *SCL* gene encodes a highly conserved, tightly regulated, tissue-specific transcription factor that is expressed in hemangioblast-derived hematopoietic and vascular endothelial cells and specific regions of the central nervous system (19). We utilized *Scl*-Cre-ERT2 transgenic mice to induce *Vhl* deletion in hemangioblast lineages. The conditional knockout allele of *Vhl* carries two loxP sites flanking exon1 of the *Vhl* gene (11). To determine the Cre expression pattern, we bred the *Scl*-Cre-ERT2 mice with *Rosa26*-AP reporter mice (17). We then administrated tamoxifen (2 mg/40 g body weight) in the *Scl*-Cre-ERT2;*Rosa26*-AP mice for five consecutive days starting at postnatal day 14. AP staining of harvested retinas exhibited strong AP activity within the retinal vasculature of tamoxifen-treated 3-month-old *Scl*-Cre-ERT2; *Rosa26*-AP mice (Fig. 1A and B), confirming Cre expression in hemangioblast-derived cells.

Next, we induced the *Vhl* deletion in *Scl*-Cre-ERT2; $Vhl^{F/F}$ mice using tamoxifen as described above. PCR showed that the *Vhl* deletion band was only detected in the retinas of 2-month-old tamoxifen-treated *Scl-Cre-ERT2;* $Vhl^{F/F}$ mice (*Vhl* CKO mice; Fig. 1C and D). Compared with the tamoxifen-treated littermate control ($Vhl^{F/F}$), Western blot analysis confirmed decreased VHL protein in the retinas of 2.5-month-old *Vhl*-mutant mice (Fig. 1E). To confirm upregulated HIF pathways in the mutant retina, we checked the expression level of *Ca9*, a well-known HIF down-stream gene. As expected, the CA9 protein level was significantly higher in the *Vhl*-mutant retinas than littermate controls (Fig. 1E).

Vhl deletion leads to retinal vascular defects consistent with ocular VHL disease

Funduscopic examination of the *Vhl* CKO mice was performed by indirect ophthalmoscopy starting 2 months following tamoxifen treatment. Compared with the normal appearing fundus of control mice, 64% (18/28) of 5-month-old *Vhl* CKO mice exhibited at least one of the following retinal vascular anomalies (Fig. 2A–E): persistent fetal vasculature (PFV) in the vitreous (n = 13, 46%; Fig. 2A), retinal vascular defects with prominent tortuous retinal vasculature, neovasculature, and/or hemorrhage (n = 6, 21%; Fig. 2B), and retinal red or grayish lesions (n = 7, 25%; Fig. 2C and D). All of these retinal vascular anomalies occurred in both male and female mutant mice (Fig. 2F). The dilated tortuous vessels and retinal red or grayish lesions are very similar with the initial appearance of RCH in patients with VHL (20).

Compared with the littermate control mice, histologic analysis of the *Vhl* CKO mice with PFV confirmed persistence of fetal hyaloid arteries in thirteen 5-month-old *Vhl* CKO mice (Fig. 3A–F). Residual degenerative hyaloid vessels adherent to the posterior capsule of the lens were also evident in 46% (6/13) of the affected mice (Fig. 3G). These results indicate that lack of pVHL in the mouse retinal vasculature disrupts the programmed regression of hyaloid vessels. PFV is very rare in VHL patients. This may be due to the regression of the fetal hyaloid artery during the third trimester, prior to loss of heterozygosity of *VHL*. In mice, hyaloid artery completely regresses about 3 weeks after birth, later than the tamoxifen treatment.

We monitored the progression of RCH-like lesions including dilated tortuous vessels (Fig. 4A) and retinal red or grayish lesions in nine *Vhl* CKO mice until 9 months of age. Except for severe hemorrhage in one 3-month-old *Vhl* CKO mouse (Fig. 4B), the dilated tortuous vasculature remained stable, and unlike the RCH lesions of human VHL patients, the retinal RCH-like lesions did not develop into large tumors in mice. To check whether these lesions lead to leakage of retinal hard exudate as human RCH, we performed FA with four 4- to 6-month-old *Vhl* CKO mice with dilated tortuous vessels. Bright-field images confirmed the funduscopic results with dilated tortuous vessels and other retinal lesions in all of the four *Vhl* CKO mice (Fig. 4C and D). FA images also revealed increased vascular permeability, leakage, and anomalous capillary networks in all of the four *Vhl* CKO mice, compared with the littermate controls (Fig. 4E and F).

We further performed histologic analysis of five 6- to 9- month-old *Vhl* CKO mice with RCH-like lesions and identified occasional foamy stromal cells (“tumorlet” cells) and “tumorlet” cell clusters around dilated vessels in all of the five *Vhl* CKO mice (Fig. 5A–D). These findings are similar with pre-tumor hemangioblast cell clusters observed during RCH development in VHL patients (2, 21–23). To prove that these “tumorlet” cells are derived from *Scl*-Cre-ERT2-mediated *Vhl* mutant hemangioblast cell lineage, we also performed IHC staining of CD31, SCL, and VEGF on the adjacent slides. CD31 and SCL positive cells can be identified in the “tumorlet” cell clusters (Fig. 5C and E). Compared with the littermate control, VEGF protein level was also significantly increased in the “tumorlet” cells around the dilated vessels (Fig. 5F and G). These results suggest that *Scl*-Cre-ERT2-mediated *Vhl* deletions in mouse retinas can mimic the early stages of human hemangioblastoma development.

LOH of the *VHL* tumor suppressor gene is necessary for hemangioblastoma tumorigenesis (1). To further determine whether the "tumorlet" cells identified above carry the *Vhl* deletion, we isolated the "tumorlet" cell cluster using laser capture microdissection and extracted DNA from micro-dissected cells (Fig. 6A–C). The cells isolated from the nearby inner nuclear layer of the retina serve as control sample. Nested PCR demonstrated that the *Vhl* deletion was only present in the "tumorlet" cells, but not in control cells (Fig. 6D and E).

Vhl deletion leads to hemangioblastoma-like lesions in mouse brainstem

Because hemangioblastomas of the brainstem, cerebellum, and spinal cord are common in patients with VHL disease, we also analyzed our *Vhl* CKO mice for CNS hemangioblastomas. AP staining of the 3-month-old tamoxifen-treated *Scl*-Cre-ERT2;*Rosa26*-AP reporter mice revealed potent Cre activity in cerebellum and brainstem vasculature (Fig. 7A and B). Although MRI failed to detect any neoplasms of the brainstem or spinal cord in six 1-year-old *Vhl* CKO mice, histologic analysis of the cerebellum and brainstem revealed dilated vasculature in the brainstems of all of the six examined mice (Fig. 7C and D). "Tumorlet" cells around dilated vessels of the brainstem were apparent in two out of six examined mice (Fig. 7D). Our results indicate that *Scl*-Cre-ERT2-mediated *Vhl* deletion may also contribute to the development of CNS hemangioblastoma in mice.

Beyond the retina and brain, we did not find any specific lesions in the kidney and pancreas of our *Vhl*-mutant mice, which is consistent with prior reports that the tumor cells of origin in the kidney and pancreas of VHL are not hemangioblast derived (9).

Discussion

Hemangioblastomas are one of the most common tumors to afflict patients with VHL disease, occurring in over 60% of VHL patients (2, 3). RCH is the first manifestation of the disorder in almost half of the patients (9). Although the majority of patients with VHL disease have good vision in at least one globe, approximately 1 in 20 patients will be legally blind. Indeed, VHL disease causes significant ocular morbidity with 10% of affected globes eventually requiring enucleation (5). Laser photocoagulation and cryotherapy are the mainstays of treatment for ocular VHL, but are limited by the destructive effects on normal eye structures and by incomplete responses in large lesions (9, 24). Thus, the development of novel treatment strategies for ocular VHL is warranted.

The current understanding of the pathogenesis of RCHs is limited, thereby potentially explaining the underwhelming success of nonablative treatments such as anti-VEGF agents (25–27). Despite of general understanding of the cellular effects of VHL protein dysfunction or absence, rational design of therapy for RCHs has been impeded by lack of a testable model for pathogenesis and progression. Thus, animal models of RCH are paramount for guiding future preclinical therapeutic investigations while providing a platform for the further study of hemangioblastoma oncogenesis *in vivo*.

Until now, no *Vhl*-mutant mice have been reported to develop RCHs. In this study, we used *Scl*-Cre-ERT2 transgenic mice to generate conditional *Vhl* deletion in hemangioblast

derived tissues after birth. More than half of the mutant mice exhibited funduscopic and histologic evidence of prominent abnormal retinal vasculature and “tumorlet” cells in the mutant retinas. The pathologic changes observed in the mutant mice are consistent with RCH observed in VHL patients (5, 20, 23). According to our knowledge, this is the first VHL disease mouse model with human VHL hemangioblastoma-like lesions.

In 2010, van Rooijen and colleagues reported that biallelic inactivation of *Vhl* led to increased vascular permeability, neovascularization, and macular edema in the retina of zebrafish (6). The neovascularization observed in their model is similar to the vascular changes observed in the retinas of our mutant mice. Indeed, isolated retinal neovascularization without concurrent hemangioblastoma has been reported in approximately 8% of VHL patients (20, 28). Thus, our model reproduces both RCHs and retinal neovascularization, which are observed in VHL patients.

As hemangioblastomas are heterogeneous tumors containing both proliferative endothelial and neoplastic stromal cells, the cell of origin of these tumors has been a subject of ongoing debate (2, 3). In 2007, Park and colleagues reported that hemangioblastoma cells cultured *in vitro* express FLK1 and brachyury, and are able to be differentiated into erythrocytes, granulocytes, and endothelial cells, suggesting that the neoplastic stromal cells are derived from embryonically arrested hemangioblasts (16). Hemangioblasts are mesoderm-derived multipotent precursors that transiently express SCL, and can differentiate into both hematopoietic and endothelial cell lineages (29). In our model, *Scl*-Cre-ERT2 transgenic mice enable conditional *VHL* deletion in cells derived from the hemangioblast (19). Kurihara and colleagues used Cre transgenic mice driven by the *Pax6* retina-specific regulatory element α-promoter (*α-Cre*) to conditionally knockout *Vhl* in retinal neural progenitor cells (15). Although these transgenic mice had persistent fetal hyaloid vasculature, they failed to develop retinal RCH-like vascular lesions. The formation of RCH-like abnormalities in our *Scl*-Cre-ERT2; $Vhl^{F/F}$ mice provides the first *in vivo* evidence that the neoplastic cells that give rise to hemangioblastomas may be derived from the hemangioblast lineage. Although investigation into the pathogenesis of hemangioblastoma is warranted, our data suggest that hemangioblast-derived cells with *Vhl* mutation have the potential to form hemangioblastomas in the eye and brain.

In conclusion, we describe the first VHL mouse disease model of RCH, and provide the *in vivo* evidence that hemangioblastomas are derived from hemangioblast cells. We anticipate that this model will support future investigations examining the oncogenesis of retinal and CNS hemangioblastomas and their treatment.

Acknowledgments

We thank Dr. Tudor Badea from NEI for kindly gifting the *Rosa26*-AP reporter mice and offering the detailed guidance with AP staining. We thank Dr. Robert Fariss of NEI Bioimaging Core for the help with MicronIII imaging system and microdissection procedures. This work was supported by the Intramural Research Program of National Eye Institute (NEI), National Cancer Institute (NCI), and National Institute of Neurological Disorders and Stroke (NINDS) at NIH (Bethesda, MD). The grant numbers are: ZIA EY000222–30 (to C.-C. Chan), ZIC EY000461–8 (to C.-C. Chan), and ZIA EY000514–06 (to E.Y. Chew).

References

1. Gossage L, Eisen T, Maher ER. VHL, the story of a tumour suppressor gene. Nat Rev Cancer 2015;15:55–64. [PubMed: 25533676]
2. Lonser RR, Glenn GM, Walther M, Chew EY, Libutti SK, Linehan WM, et al. von Hippel-Lindau disease. Lancet 2003;361:2059–67. [PubMed: 12814730]
3. Butman JA, Linehan WM, Lonser RR. Neurologic manifestations of von Hippel-Lindau disease. JAMA 2008;300:1334–42. [PubMed: 18799446]
4. Latif F, Tory K, Gnarra J, Yao M, Duh FM, Orcutt ML, et al. Identification of the von Hippel-Lindau disease tumor suppressor gene. Science 1993;260: 1317–20. [PubMed: 8493574]
5. Wong WT, Agron E, Coleman HR, Tran T, Reed GF, Csaky K, et al. Clinical characterization of retinal capillary hemangioblastomas in a large population of patients with von Hippel-Lindau disease. Ophthalmology 2008;115:181–8. [PubMed: 17543389]
6. van Rooijen E, Voest EE, Logister I, Bussmann J, Korving J, van Eeden FJ, et al. von Hippel-Lindau tumor suppressor mutants faithfully model pathological hypoxia-driven angiogenesis and vascular retinopathies in zebrafish. Disease Models Mech 2010;3: 343–53.
7. Tarade D, Ohh M. The HIF and other quandaries in VHL disease. Oncogene 2017;37:139–47. [PubMed: 28925400]
8. Maher ER, Neumann HP, Richard S. von Hippel-Lindau disease: a clinical and scientific review. Eur J Hum Gen 2011;19:617–23.
9. Park S, Chan CC. Von Hippel-Lindau disease (VHL): a need for a murine model with retinal hemangioblastoma. Histol Histopath 2012; 27:975–84.
10. Rankin EB, Tomaszewski JE, Haase VH. Renal cyst development in mice with conditional inactivation of the von Hippel-Lindau tumor suppressor. Cancer Res 2006;66:2576–83. [PubMed: 16510575]
11. Haase VH, Glickman JN, Socolovsky M, Jaenisch R. Vascular tumors in livers with targeted inactivation of the von Hippel-Lindau tumor suppressor. Proc Nat Acad Sci U S A 2001;98:1583–8.
12. Ma W, Tessarollo L, Hong SB, Baba M, Southon E, Back TC, et al. Hepatic vascular tumors, angiectasis in multiple organs, and impaired spermatogenesis in mice with conditional inactivation of the VHL gene. Cancer Res 2003;63:5320–8. [PubMed: 14500363]
13. Frew IJ, Thoma CR, Georgiev S, Minola A, Hitz M, Montani M, et al. pVHL and PTEN tumour suppressor proteins cooperatively suppress kidney cyst formation. EMBO J 2008;27:1747–57. [PubMed: 18497742]
14. Shen HC, Adem A, Ylaya K, Wilson A, He M, Lorang D, et al. Deciphering von Hippel-Lindau (VHL/Vhl)-associated pancreatic manifestations by inactivating Vhl in specific pancreatic cell populations. PLoS One 2009; 4:e4897. [PubMed: 19340311]
15. Kurihara T, Kubota Y, Ozawa Y, Takubo K, Noda K, Simon MC, et al. von Hippel-Lindau protein regulates transition from the fetal to the adult circulatory system in retina. Development 2010;137:1563–71. [PubMed: 20388654]
16. Park DM, Zhuang Z, Chen L, Szerlip N, Maric I, Li J, et al. von Hippel-Lindau disease-associated hemangioblastomas are derived from embryologic multipotent cells. PLoS Med 2007;4:e60. [PubMed: 17298169]
17. Badea TC, Hua ZL, Smallwood PM, Williams J, Rotolo T, Ye X, et al. New mouse lines for the analysis of neuronal morphology using CreER(T)/loxP-directed sparse labeling. PloS One 2009;4:e7859. [PubMed: 19924248]
18. Paques M, Guyomard JL, Simonutti M, Roux MJ, Picaud S, Legargasson JF, et al. Panretinal, high-resolution color photography of the mouse fundus. Investigative Ophthalmol Visual Sci 2007;48:2769–74.
19. Elefanty AG, Begley CG, Hartley L, Papaevangeliou B, Robb L. SCL expression in the mouse embryo detected with a targeted lacZ reporter gene demonstrates its localization to hematopoietic, vascular, and neural tissues. Blood 1999;94:3754–63. [PubMed: 10572089]
20. Chew EY. Ocular manifestations of von Hippel-Lindau disease: clinical and genetic investigations. Trans Am Ophthalmol Soc 2005;103:495–511. [PubMed: 17057815]

21. Chan CC, Collins AB, Chew EY. Molecular pathology of eyes with von Hippel-Lindau (VHL) Disease: a review. Retina 2007;27:1–7. [PubMed: 17218907]
22. Chen S, Chew EY, Chan CC. Pathology characteristics of ocular von Hippel-Lindau disease with neovascularization of the iris and cornea: a case report. J Med Case Rep 2015;9:66. [PubMed: 25885645]
23. Chan CC, Chew EY, Shen D, Hackett J, Zhuang Z. Expression of stem cells markers in ocular hemangioblastoma associated with von Hippel-Lindau (VHL) disease. Mol Vision 2005;11:697–704.
24. Haddad NM, Cavallerano JD, Silva PS. Von hippel-lindau disease: a genetic and clinical review. Semin Ophthalmol 2013;28:377–86. [PubMed: 24138046]
25. von Buelow M, Pape S, Hoerauf H. Systemic bevacizumab treatment of a juxtapapillary retinal haemangioma. Acta Ophthalmol Scand 2007;85: 114–6. [PubMed: 17244223]
26. Rosenblatt MI, Azar DT. Anti-angiogenic therapy: Prospects for treatment of ocular tumors. Semin Ophthalmol 2006;21:151–60. [PubMed: 16912013]
27. Aiello LP, George DJ, Cahill MT, Wong JS, Cavallerano J, Hannah AL, et al. Rapid and durable recovery of visual function in a patient with von hippel-lindau syndrome after systemic therapy with vascular endothelial growth factor receptor inhibitor su5416. Ophthalmology 2002; 109:1745–51. [PubMed: 12208726]
28. Wong WT, Yeh S, Chan CC, Kalina RE, Kinyoun JL, Folk JC, et al. Retinal vascular proliferation as an ocular manifestation of von Hippel-Lindau disease. Arch Ophthalmol 2008;126:637–43. [PubMed: 18474773]
29. Psaltis PJ, Harbuzariu A, Delacroix S, Holroyd EW, Simari RD. Resident vascular progenitor cells-diverse origins, phenotype, and function. J Cardiovasc Transl Res 2011;4:161–76. [PubMed: 21116882]

Significance:

This study describes a model that phenotypically recapitulates a form of retinal pathogenesis that is driven by genetic loss of the VHL tumor suppressor, providing a useful tool for its study and therapeutic intervention.

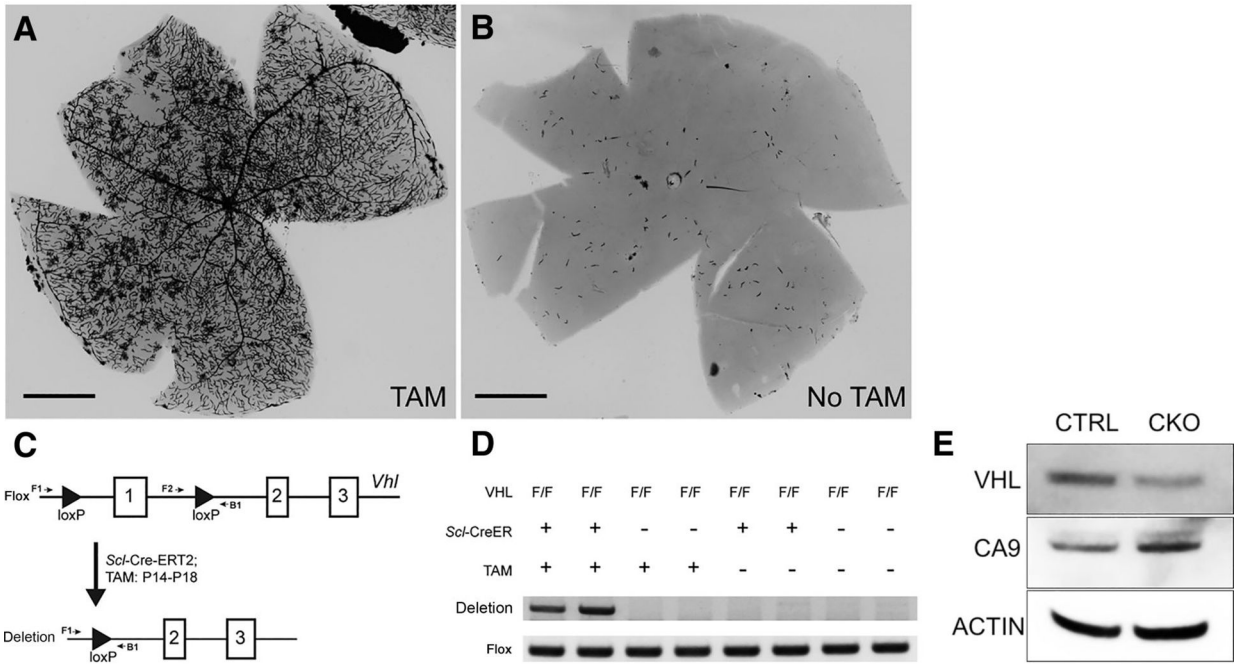

Figure 1.

Efficient *Vhl* deletion in retinal vasculature system. **A,** AP staining of the whole retina isolated from 3-month-old *Scl*-Cre-ERT2;*Rosa26*-AP mice with tamoxifen treatment (TAM). Robust Cre activity is detected in the retinal vasculature system. **B,** Rare Cre activity was detected in 3-month-old *Scl*-Cre-ERT2; *Rosa26*-AP mice without tamoxifen treatment. **C,** Diagram of *Vhl* conditional knockout system by *Scl*-Cre-ERT2 with tamoxifen treatment. PCR with F2/B1 was used to identify the conditional allele, whereas PCR with F1/B1 was used to identify the *Vhl* deletion allele. **D,** Genotyping PCR with retinal DNA of 2-month-old mice with indicated genotype and treatment. Two mice of each genotype and treatment were examined. Negative images of ethidium bromide-stained gels are shown. *Vhl* deletion allele was only identified in the retinas of *Scl*-Cre-ERT2; $Vhl^{F/F}$ mice with tamoxifen injection. Flox allele band (F2/R1) served as an internal control. **E,** Western blot analysis of VHL, CA9, β-actin with retinal protein of 2.5-month-old tamoxifen-treated littermate control (CTRL, $Vhl^{F/F}$), and *Vhl* conditional knockout (CKO, *Scl*-Cre-ERT2; $Vhl^{F/F}$) mice. Scale bars for **A** and **B**, 1 mm.

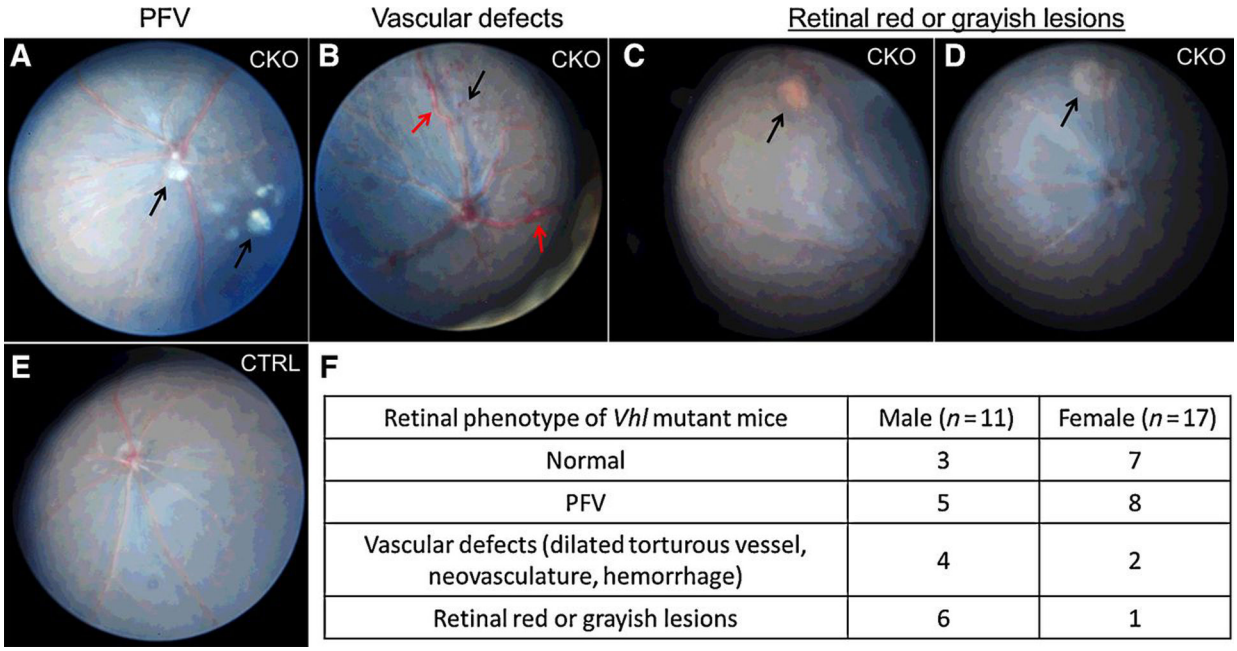

Retinal phenotype of *Vhl* mutant mice	Male ($n=11$)	Female ($n=17$)
Normal	3	7
PFV	5	8
Vascular defects (dilated torturous vessel, neovasculature, hemorrhage)	4	2
Retinal red or grayish lesions	6	1

Figure 2.

Summary of funduscopic images of 5-month-old *Vhl* CKO mice. Representative funduscopic images of 5-month-old *Vhl* CKO mice are shown in **A**–**D**. **A,** PFV in the vitreous. Black arrows, remnant hyaloid vessels. **B,** Vascular defects, including dilated tortuous vessel (red arrows), and neovasculature (black arrow). **C,** RCH-like lesions with retinal hemorrhage (arrow). **D,** Retinal grayish lesion (arrow). **E,** Normal fundus in littermate control mice. **F**, Summary of the funduscopic results of 28 5-month-old *Vhl* CKO mice.

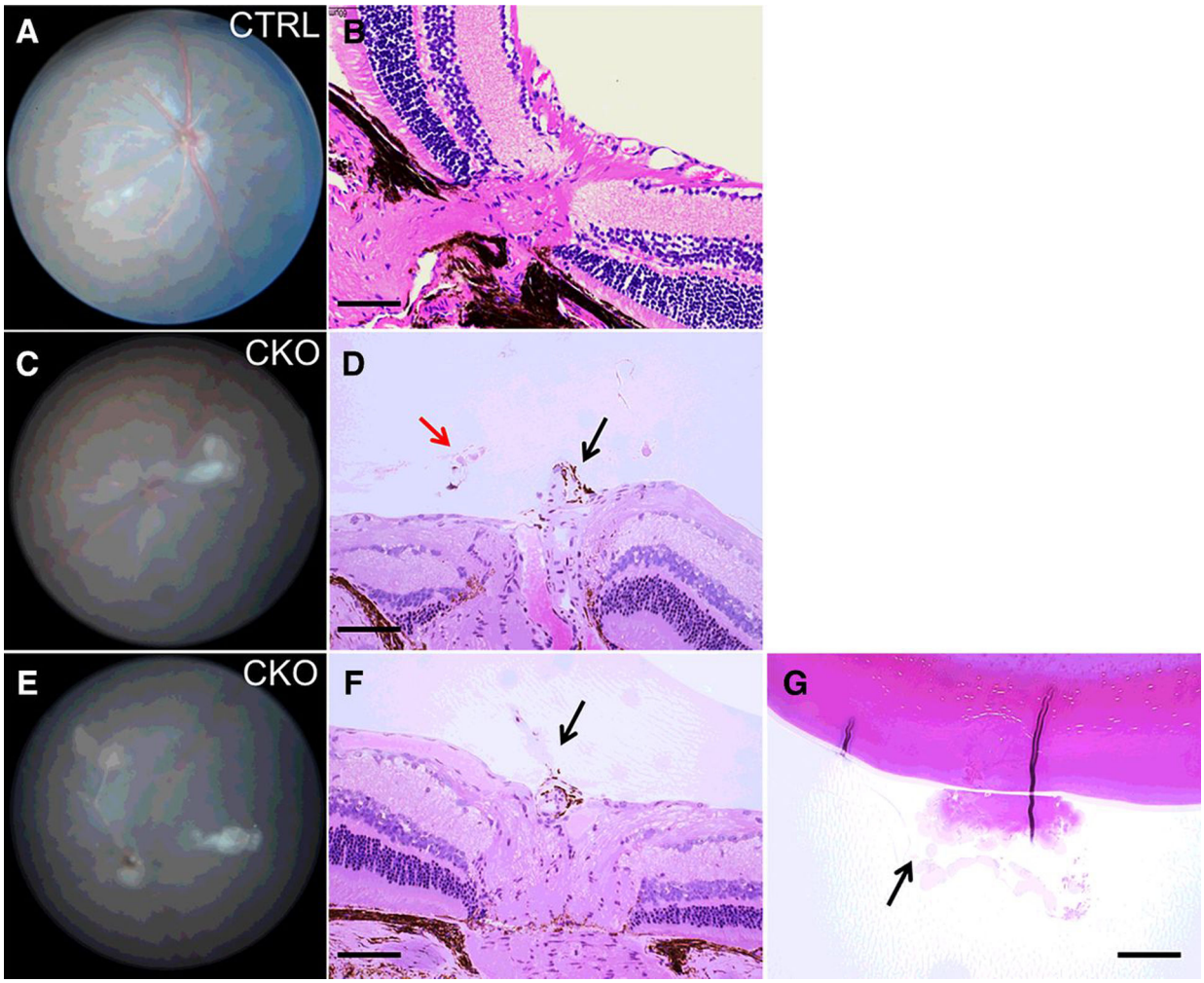

Figure 3.

Histologic analysis of *Vhl*-mutant mice reveals PFV. **A** and **B,** Funduscopic and histologic images of a 5-month-old control mouse. The hyaloid artery has completely regressed. **C** and **D,** Representative funduscopy and histologic images of a 5-month-old *Vhl*-mutant mouse. Black arrow, persistent hyaloid vessel; red arrow, retinal neovascularization in the vitreous. **E–G,** Another *Vhl*-mutant mouse of similar age exhibited persistent hyaloid vessel (**F**, arrow), and vitreous fibro-neovascular structure adherent to the lens (**G**, arrow). Scale bars for **B**, **D**, **F**, **G**, 100 μm.

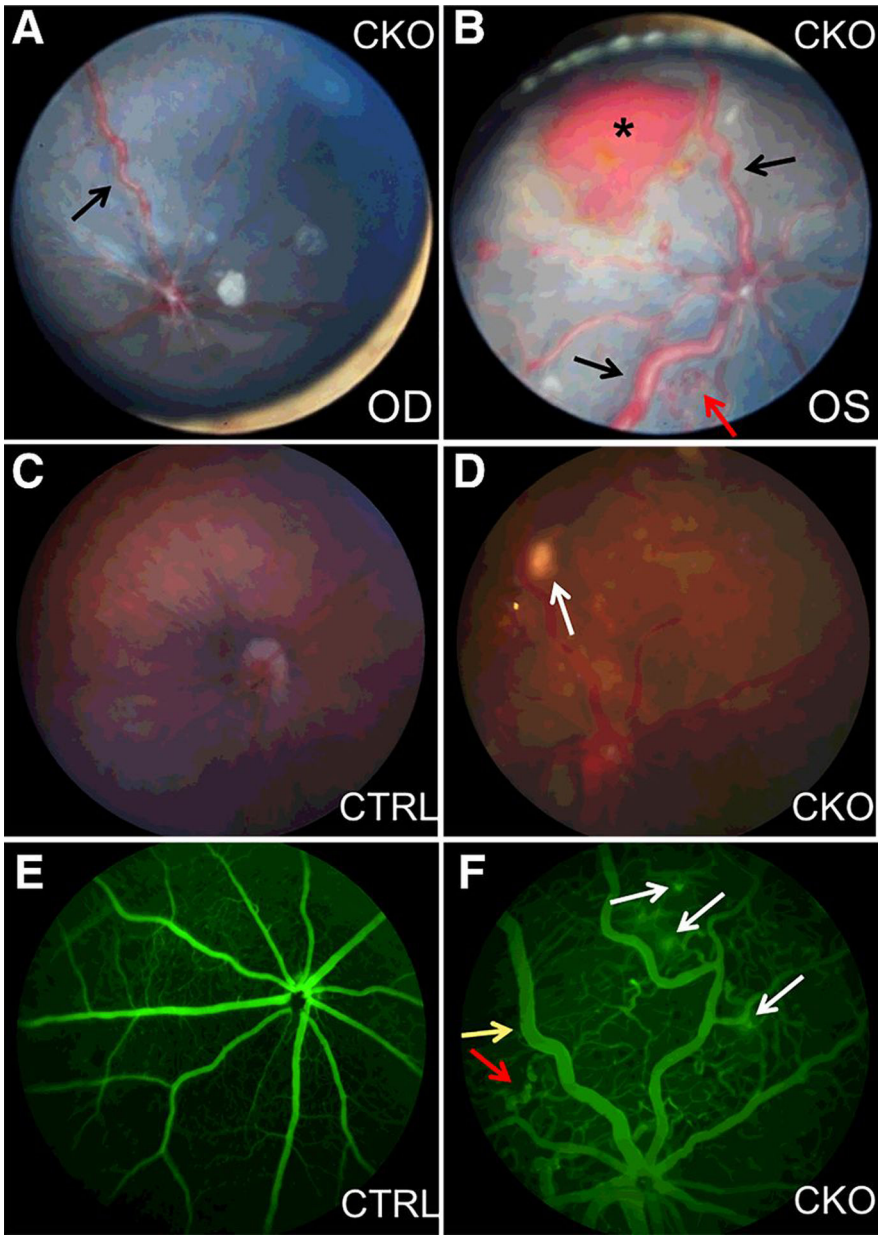

Figure 4.

Prominent vasculature, anomalous capillary networks, and hemorrhage in *Vhl* mutants. **A** and **B,** Representative funduscopic images reveal tortuous and dilated vessels (black arrows) in both eyes of a 3-month-old *Vhl* CKO mouse. Hemorrhage (asterisk) and neovascular tufts (red arrow) can also be found in the left eye. OD, right eye; OS, left eye. **C,** Representative bright-field image (Micron III imaging system) of a 4-month-old control mouse. **D,** Representative bright-field image shows RCH-like lesion (arrow) and abnormal vessels in a 4-month-old *Vhl* mutant mouse. **E,** FA with Micron III imaging system shows normal retinal vasculature in the 4-month-old control mouse. **F,** FA shows dilated tortuous vessels (yellow arrow), anomalous capillary networks (red arrow), and leakage (white arrows) in the 4-month-old *Vhl* CKO mouse.

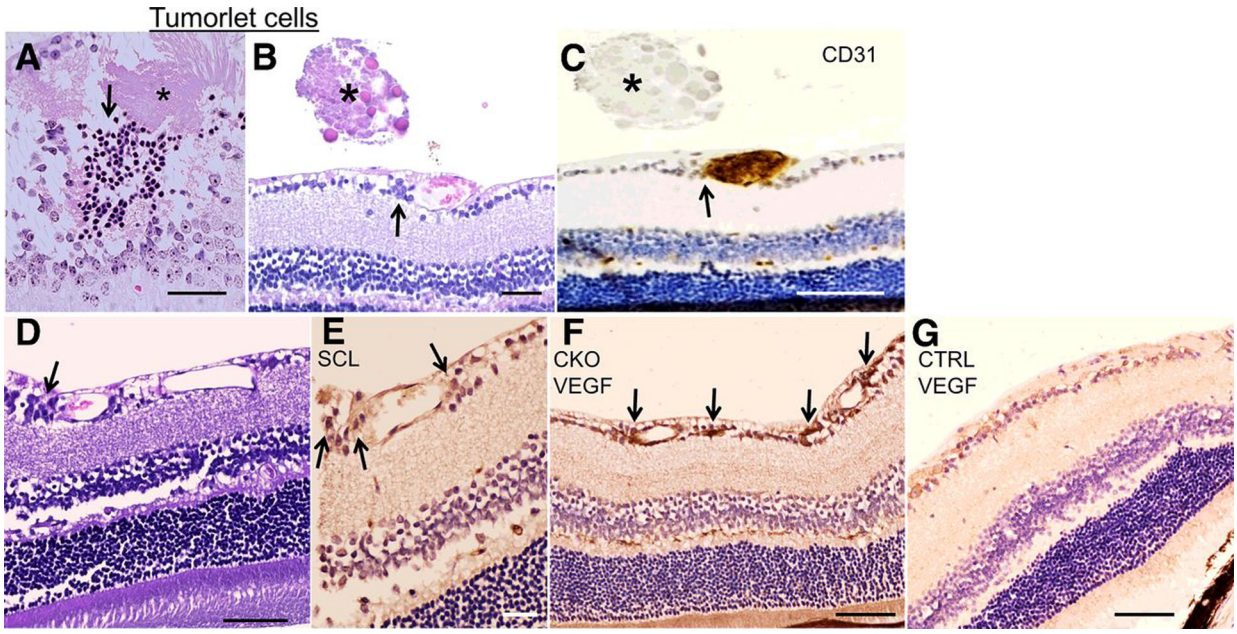

Figure 5.

Characterization of the "tumorlet" cells in *Vhl* CKO mice. **A,** Representative histologic image shows a cluster of "tumorlet" cells (arrow) adjacent to an old retinal hemorrhage (asterisk) in a 7-month-old *Vhl* CKO mouse. **B** and **D,** Representative H&E images reveal "tumorlet" cells (arrow) adjacent to the dilated vessels. Asterisk indicates old hemorrhage in the vitreous (**B**). **C,** IHC staining of CD31 shows CD31 positive cells (arrow) in the "tumorlet" cell clusters. **E,** IHC staining of SCL reveals SCL-positive cells (arrow) in the "tumorlet" area. **F,** IHC staining of VEGF shows upregulated VEGF expression in the dilated vessels and the adjacent "tumorlet" cells (arrows). **G**, IHC staining of VEGF on littermate control retina shows weak VEGF expression. Scale bars for **A** and **B**, 50 μm; **C**, 100 μm; **D**, **F**, **G**, 60 μm; **E**, 30 μm.

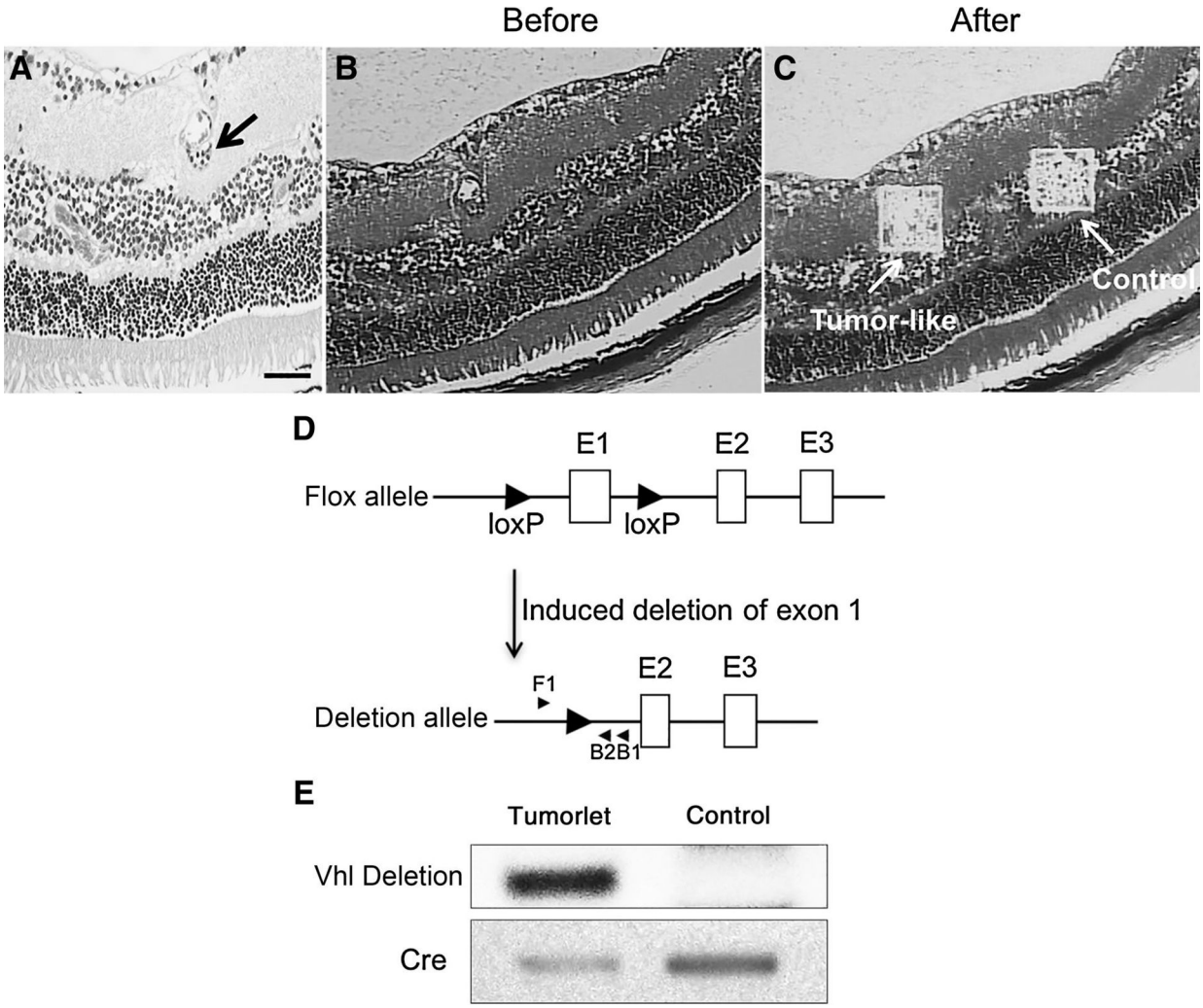

Figure 6.

The "tumorlet" cells carry *Vhl* deletion. **A,** H&E staining shows the "tumorlet" cells (arrow) for microdissection. **B** and **C**, Images before (**B**) and after (**C**) microdissection. The "tumorlet" region and control region are labeled (arrow). **D,** Diagram of the primers used for nested PCR. PCR product of F1/B1 is used as template for second-round PCR with F1/B2. **E,** PCR results of the microdissected samples. Negative images of ethidium bromide-stained gels are shown. *Vhl* deletion was only detected in the "tumorlet" cells, but not the control region. Genotyping PCR of Cre with the same amount of microdissection DNA is shown as internal control to prove adequate DNA from both "tumorlet" and control region.

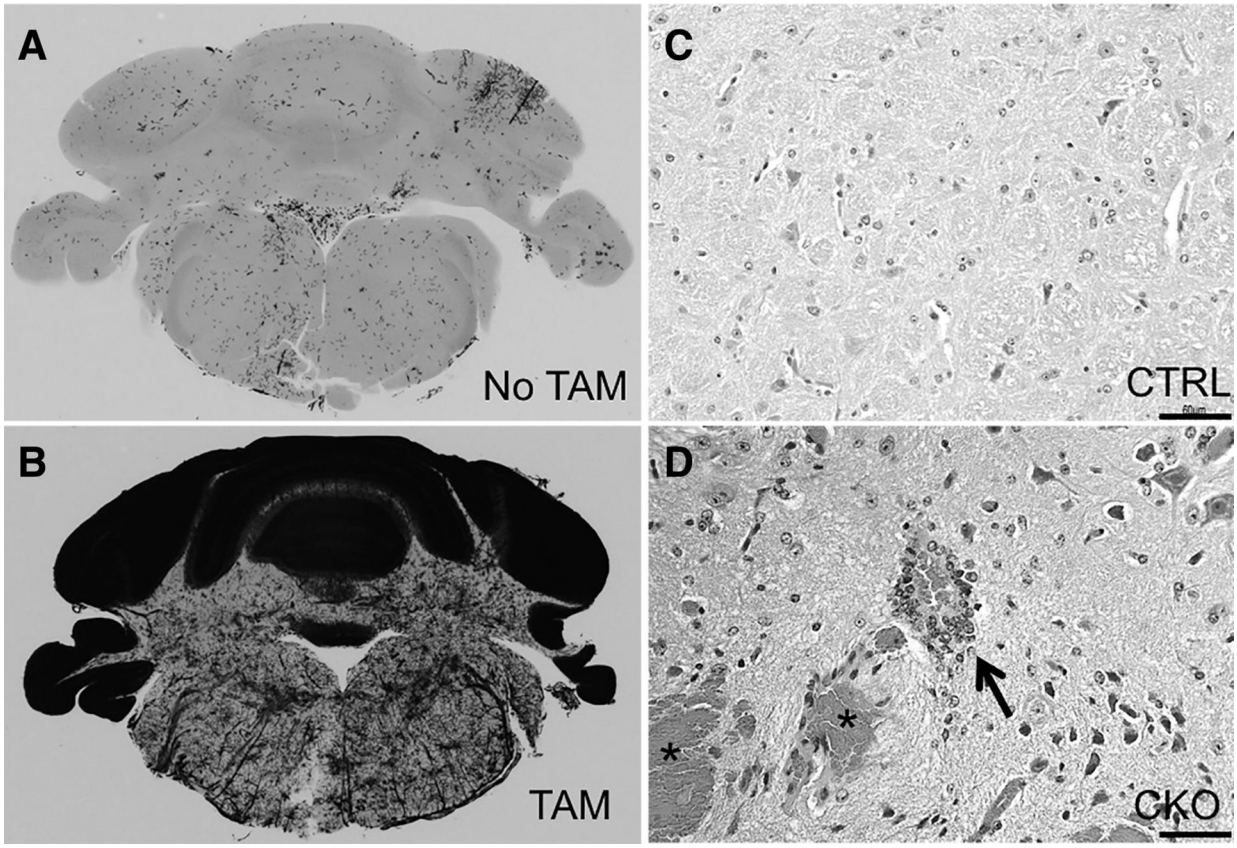

Figure 7.

CNS vasculature defects in *Vhl* CKO mice. **A** and **B,** AP staining of brains from 3-month-old *Scl*-Cre-ERT2; *Rosa26*-AP mice without (**A**) or with (**B**) tamoxifen treatment. **C,** Normal brainstem of a 1-year-old control mouse. **D,** Hemorrhages (asterisks) and "tumorlet" cells (arrow) in the brainstem of a 1-year-old mutant mouse. Scale bars for **C** and **D**, 60 μm.